effects may possibly not be entirely neglected. Nonetheless, we insist that deviations from the usual lyotropic polymer behavior due to the effect of twist should show up.

As a final comment we remark that there is an urgent need for quantitative experimental data on the isotropic–anisotropic phase transition concentrations as function of charge density and salt strengths. So far nothing of this kind is available in the literature.

References and Notes

(1) Onsager, L. *Ann. N.Y. Acad. Sci.* **1949**, *51*, 627.
(2) Zocher, H. *Z. Anorg. Chem.* **1925**, *147*, 91.
(3) Zocher, H.; Török, C. *Kolloid-Z.* **1960**, *170*, 140; **1960**, *173*, 1; **1962**, *180*, 41.
(4) Bugosh, J. *J. Phys. Chem.* **1961**, *65*, 1791.
(5) Bernal, J. D.; Frankuchen, I. *J. Gen. Physiol.* **1941**, *25*, 111.
(6) Oster, G. *J. Gen. Physiol.* **1950**, *33*, 445.
(7) Gregory, J.; Holmes, K. C. *J. Mol. Biol.* **1965**, *13*, 796.
(8) Kreibig, U.; Wetter, G. *Z. Naturforsch., C: Biosci.* **1980**, *35C*, 750.
(9) Fraden, S.; Hurd, A. J.; Meyer, R. B.; Cahoon, M.; Caspar, D. L. D. *J. Phys. (Les Ulis, Fr.)* **1985**, *46*, C3–85.
(10) Brian, A. A.; Frisch, H. L.; Lerman, L. S. *Biopolymers* **1981**, *20*, 1305.
(11) Rill, R. L.; Hilliard, P. R.; Levy, G. C. *J. Biol. Chem.* **1983**, *28*, 250.
(12) Marchessault, R. H.; Morehead, F. F.; Walter, N. M. *Nature (London)* **1959**, *184*, 632.
(13) Itou, T.; Teramoto, A. *Polym. J. (Tokyo)* **1982**, *14*, 999; **1984**, *16*, 779.
(14) Yanaki, T.; Norisuye, T.; Teramoto, A. *Polym. J. (Tokyo)* **1984**, *16*, 165.
(15) Perutz, H. F.; Liquori, A.; Eirich, F. *Nature* **1951**, *167*, 929.
(16) Allison, A. C. *Biochem. J.* **1957**, *65*, 212.
(17) Brenner, S. L.; Parsegian, V. A. *Biophys. J.* **1974**, *14*, 327.
(18) Stigter, D. *Biopolymers* **1977**, *16*, 1435.
(19) Fixman, M.; Skolnick, J. *Macromolecules* **1978**, *11*, 863.
(20) Lekkerkerker, H. N. W.; Coulon, Ph.; Haegen, van der R.; Deblieck, R. *J. Chem. Phys.* **1984**, *80*, 3427.
(21) Straley, J. P. *Phys. Rev. A* **1973**, *8*, 2181.
(22) Khokhlov, A. R.; Semenov, A. N. *Macromolecules* **1984**, *17*, 2678.
(23) Odijk, T.; Lekkerkerker, H. N. W. *J. Phys. Chem.* **1985**, *89*, 2090.
(24) Odijk, T. *Polym. Commun.* **1985**, *26*, 197.
(25) Olver, F. W. J. *Asymptotics and Special Functions*; Academic: New York, 1974.
(26) Abramowitz, M.; Stegun, I. A. *Handbook of Mathematical Functions*; Dover: New York, 1970.
(27) McQuarrie, D. A. *Statistical Mechanics*; Harper, and Row: New York, 1976.
(28) Hill, T. L. *Arch. Biochem. Biophys.* **1955**, *57*, 229.
(29) Derjaguin, B. *Kolloid-Z.* **1934**, *69*, 155.
(30) Fixman, M. *J. Chem. Phys.* **1979**, *70*, 4995.
(31) Philip, J. R.; Wooding, R. A. *J. Chem. Phys.* **1970**, *52*, 953.
(32) Russel, W. B. *J. Polym. Sci., Polym. Phys. Ed.* **1982**, *20*, 1233.
(33) Odijk, T. *Chem. Phys. Lett.* **1983**, *100*, 145.
(34) Lampert, M. A.; Crandall, R. S. *Chem. Phys. Lett.* **1980**, *72*, 481.
(35) Lee, S. N.; Meyer, R. B. *J. Chem. Phys.* **1986**, *84*, 3443.

Dielectric Relaxation in Poly(ethylene terephthalate)

John C. Coburn† and Richard H. Boyd*

Department of Materials Science and Engineering and Department of Chemical Engineering, University of Utah, Salt Lake City, Utah 84112.

Received March 17, 1986

ABSTRACT: Dielectric constant and loss have been measured over the frequency range 1 Hz to 100 kHz over a wide temperature range for a series of poly(ethylene terephthalate) (PET) specimens spanning the crystallinity range from essentially amorphous to 62%. The higher crystallinities were achieved via crystallization under pressure. Previous work has indicated that the β subglass process does not extrapolate to zero relaxation strength at 100% crystallinity. Taking advantage of higher crystallinities (and the knowledge that the crystalline density on which some previous crystallinity scales have been based was not completely reliable) we demonstrate here that both the α_a glass–rubber relaxation and the β process extrapolate to zero strength at a density corresponding to 100% crystallinity. This indicates amorphous-phase origin for both processes. The effect of crystallinity on the relaxation parameters for these amorphous-phase processes is discussed. Interpretation of the relaxation strengths in terms of the Onsager–Kirkwood dipolar correlation factor shows that immobilization of amorphous chain segments by connections to the crystals can be detected not only by perturbation of relaxation times but by availability of configurations as well. Specific volumes of the specimens were measured as a function of temperature, and the correlation between the dielectric relaxation results and thermal expansion changes through the relaxation regions is discussed.

Introduction

Poly(ethylene terephthalate) (PET) has served as an important model for studying relaxation processes in semicrystalline polymers.[1-5] The circumstance that it can be quenched into the completely amorphous state as well as isothermally crystallized has allowed direct measurement of the effect of crystallinity presence on relaxations. PET shows two relaxation processes, one designated α_a and the other β. The former is the glass transition (disappearance of long-range segmental motion with lowering temperature) in the completely amorphous material or in the amorphous fraction in semicrystalline specimens. The α_a relaxation is quite sensitive to the presence of the crystalline fraction in that it is dramatically broader in the frequency domain and shifted to higher temperature isochronally in crystalline samples. The β relaxation, occurring at lower temperatures isochronally than the α_a process, has been thought to take place largely in the amorphous phase also and therefore is a "subglass" process. The β relaxation is insensitive to morphology, having virtually the same characteristics (other than strength or intensity) in completely amorphous materials as in semicrystalline ones. This is consonant with the molecular motions associated with it being of shorter range character than those for the α_a process. However, the assignment of the β relaxation as a *purely* amorphous one has been compromised by extrapolation of relaxation strength vs. density to 100% crystallinity. On extrapolation of their β-process strength data Ishida et al.[2] concluded that the process did not disappear at 100% crystallinity. They

† Present address: Polymer Products Department, Experimental Station, E. I. du Pont de Nemours and Co., Wilmington, DE 19898.

0024-9297/86/2219-2238$01.50/0

proposed that a third component, intermediate between the crystal and amorphous phases, was present and contributed to the β process. PET does not crystallize to high crystallinity so that the extrapolation is a long one. In more recent times, it is possible to realize that the extrapolation is even more seriously complicated by uncertainty with respect to the density of the crystal phase in PET. A number of crystal density values that differ significantly have been reported.[6-9]

In the work reported here advantage has been taken of specimens of higher crystallinity than available in previous relaxation experiments in studying several issues. These include the following. It is clear that the glass–rubber relaxation in PET and other semicrystalline polymers is seriously perturbed kinetically by immobilization of amorphous chains through their attachments to the crystals. As indicated, this results in a greatly broadened relaxation time distribution and some change in the location of the relaxation center. It is not as clear to what extent this immobilization is apparent in the availability of configurations in addition to displaced relaxation times. That is, in the context of the present dielectric measurements, the question is whether the relaxed dielectric constant of the amorphous fraction (as opposed to that of the semicrystalline composite) depends on the presence or degree of crystallinity or, put another way, whether the dipole correlation factor within the amorphous phase is perturbed by the connections of the amorphous chain segments to the crystals. Answering this question requires good-quality data over a range of crystallinities and careful attention to its analysis. Another issue is that of the morphological assignment of the β process, where the resolution of the uncertainty in the extrapolation of relaxation strength is addressed. This is a important question since the assignment of single subglass type processes to multiple-phase origin has been fairly common in the literature, and its validity needs to be carefully examined. The general dependence of the relaxation parameters on crystallinity is also examined. Finally, in the experiments conducted here it was possible to measure simultaneously sample thickness and dielectric constant. Thus another question studied was the effect of crystallinity on the thermal expansion associated with the amorphous-phase relaxations.

Experimental Section

Dielectric Measurements. The "semiautomated" dielectric apparatus consisted of a transformer arm ratio bridge (General Radio 1616 precision capacitance bridge) and a microprocessor-controlled oscillator and two-phase detector (EG&G 5206 lock-in analyzer). The BCD output of the bridge was interfaced via three 16-bit ports on a parallel interface board to a laboratory computer (Charles River Data Systems LSI 11/23 based Model MF-211). The lock-in analyzer was connected to the CRDS computer through a serial line interface. The data logging from the bridge and the lock-in analyzer settings (frequency and sensitivities) were thus under control of the CRDS computer and the microprocessors in the analyzer. Operator attention is confined to observation of the unbalance signals on the detector and manual adjustment of the bridge balancing switches in response. Considerable attention is thus still required but a distinct improvement over entirely manual operation is effected. The system was found capable of satisfactory measurements from 1 Hz to 100 kHz. The lower frequency is a decade lower than the specification on the GR 1616 bridge.

Sample Cell and Thermal Expansion Measurements. The dielectric cell was constructed for these studies and was of the parallel-plate type. In addition to the sample-occupied area another active area was provided for concurrent air or "empty cell" meausrements. As suggested by the design of Yoshihara and Work[10] this was accomplished via four separate concentric rings in the lower plate. The innermost area was occupied by the sample. The gap between the inner area and second ring creates a sample area guard. The third ring provided a air-filled active region whose distance from the upper plate was controlled by the sample thickness. The gap between the second and third rings and that between the third and fourth rings provide guards for the air-filled active electrode of the third ring. The ratios of the areas of the sample and air measurement electrodes was established by calibration with the cell entirely empty. Thus the empty cell capacitance was available at all temperatures simply by measuring the air-filled electrode capacitance.

A very attractive feature of the above cell design is the fact that the actual value of the air-filled area capacitance at any temperature can be converted (after a correction for area expansion of the electrode) to distance between the plates and therefore to sample thickness. This provides a convenient and extremely sensitive way to measure the linear thermal expansion of solid specimens. For completely amorphous materials that become fluid, measurements of thermal expansion above T_g become of dubious accuracy.

The specimens used were coated with gold deposited by evaporation in a vacuum sputterer. The coated diameter on the lower side slightly exceeded that of the active center electrode so that the active area was determined by the coating rather than the diameter. A correction to the sample area was made on the basis of the linear thermal expansion measurements under the assumption of expansional isotropy.

The dielectric measurements were made isothermally at a number of frequencies in the 1 Hz to 100 kHz range (as many as 14) that were preset in the driving program in the CRDS computer. A measurement at one frequency (10.1 kHz) served to determine the empty cell capacitance and sample thickness. The temperature was increased stepwise from low temperature to high for a specimen that had been slowly cooled.

Sample Preparation and Characterization. Nine specimens ranging from amorphous to 62% percent crystallinity were studied (see below for a discussion of the densities used in establishing the crystallinity scale). Polymers were obtained from E. I. du Pont de Nemours and Co. The amorphous specimen was prepared from unoriented amorphous PET film (Mylar). The reported M_n was 19 000. Four more samples, ranging up to 50% crystallinity, were prepared from amorphous film by isothermal crystallinity on heating the glassy film to temperatures ranging from 105 to 240 °C. The samples were held at the crystallization temperature until crystallization was complete and then slowly cooled to room temperature. The remaining three samples, ranging in crystallinity from 52 to 62%, were prepared by isobaric crystallization from the melt at high pressure. These samples, prepared from amorphous pellets (reported M_n = 21 000), were slowly heated in a piston and cylinder cell[11] to temperatures which corresponded to supercoolings of ~10 °C for the pressures at which they would be crystallized.[12] Following this, they were rapidly pressurized to the crystallization pressure (ranging from 250 to 1250 atm). Then they were slowly cooled at ~1 °C/min under pressure to room temperature and the pressure was released. The samples were then annealed at 100 °C to stabilize their density. The dielectric samples were thin disks cut from the resulting molded rods with a diamond-bladed saw.

Sample crystallinities were determined by density measurements (carbon tetrachloride/toluene density gradient column) and from heat of fusion (Perkin-Elmer DSCII differential scanning calorimeter). Both methods require calibration and this requires discussion in the case of PET. The volume fraction crystallinity, χ_c, from density requires the amorphous- and crystal-phase densities ρ_a and ρ_c, respectively. The amorphous density can be measured directly and its value of 1.336 g/cm^3 is presumably reliable.[13] The crystalline density remains uncertain even though several measurements of unit cell dimensions have been reported. There seems to be agreement on the basic structure but fairly small differences in cell parameters have a significant effect on the cell volume. Probably the most widely quoted density is the original value ρ_c = 1.455 g/cm^3 of Daubney et al.[6] Kilian et al.[7] from slightly different cell parameters reported ρ_c = 1.495 g/cm^3 and this value has been used a great deal also. Fakirov et al.[8] have reported the highest value, ρ_c = 1.515 g/cm^3 and recently Starkweather et al.[9] have published a value of ρ_c = 1.475 g/cm^3.

Table I
Crystallization Conditions and Degrees of Crystallinity for PET Samples

sample	P_c,[a] atm	T_c,[b] °C	t_c, h	ρ_s, g/cm^3	$\chi_c(\rho_c)$	ΔH_s, J/g	$\chi_c(\Delta H_s)$
1				1.342	0.04		
2		105	80	1.378	0.26		
3		115	20	1.382	0.29		
4		135	11	1.389	0.33		
5		190	0.3	1.396	0.38		
6		235	0.7	1.417	0.50	57	0.46
7	250			1.419	0.52	63	0.51
8	750			1.424	0.55	70	0.56
9	1250			1.435	0.62	77	0.62

[a] Samples 1–6 were crystallized isothermally at 1-atm pressure. [b] Samples 7–9 were crystallized by slow cooling from the melt at approximately 1 °C/min.

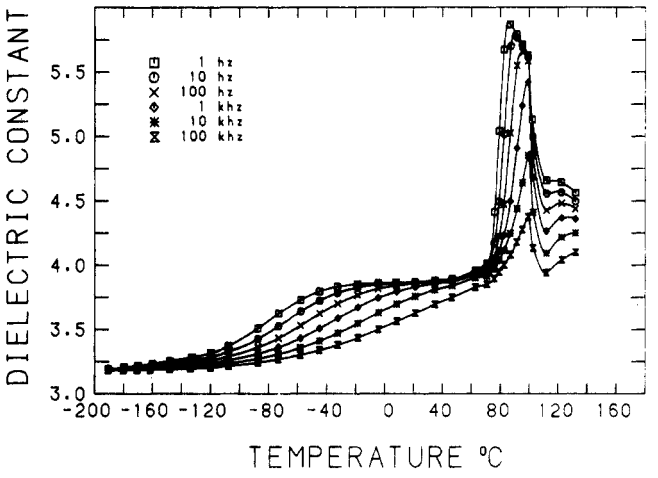

Figure 1. Dielectric constant of "amorphous" PET (sample 1, Table I, χ_c = 0.04) vs. temperature at six decade frequencies.

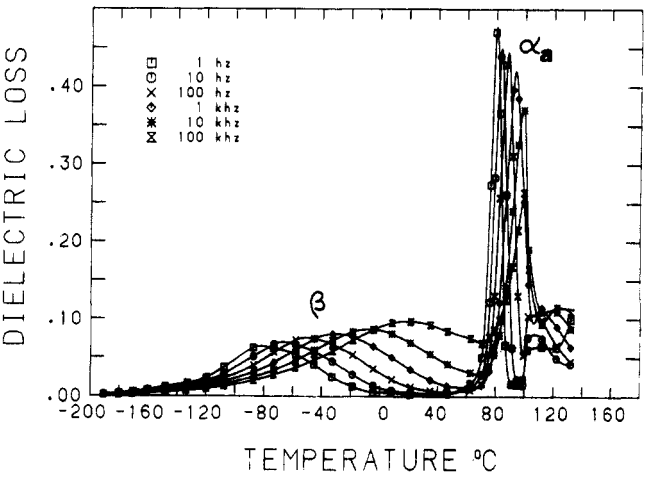

Figure 2. Dielectric loss of "amorphous" PET (sample 1, Table I, χ_c = 0.04) vs. temperuature at six decade frequencies.

These differences have a serious effect on the density crystallinity scale. For example, a specimen with a density of 1.419 g/cm^3 would have a crystallinity of 70% based on the lowest reported ρ_c above, but only 46% if based on the highest one. For reasons to be detailed below, we believe that the relaxation measurements themselves have a bearing on the crystal density and that the two middle values, those of Kilian et al.[7] and Starkweather et al.,[9] are consistent with the relaxation strength extrapolations. The Kilian et al. value of 1.495 g/cm^3 has been selected as the basis for the density crystallinities reported here. This density was the one used by Illers and Breuer[4] in their mechanical relaxation studies. Direct comparison of their reported crystallinity values and ours can be made and affords illustration of the extension of the crystallinity range here over those in previous relaxation studies. Our highest crystallinity is 62% compared to 46% in Illers and Breuer's work.

The heat of fusion measurements were calibrated against the density crystallinity of our highest crystallinity sample, and the heat of fusion value of 124 J/g for 100% crystallinity was derived. This compares with values of 136 and 115 J/g from two independent methods reported by Starkweather et al.[9] The melting points of our pressure-crystallized specimens were in the vicinity of 260 °C and not greatly different from those of the atmospheric pressure crystallized specimens. This indicates that extended-chain morphologies were not obtained. This result is similar to that of Hiramatsu and Hirakawa,[14] who found that high-pressure annealing was necessary to achieve higher melting points (see also Siegmann et al.[12]). The crystallinity characterization data are summarized in Table I. Density measurement on our "amorphous" sample actually indicates a crystallinity of 4%. We will refer to it as amorphous.

Further details with respect to all of the experimental work may be found in the Ph.D. dissertation of J.C.C.[15]

Results and Phenomenological Data Fitting

Although the dielectric data were taken in isothermal mode, it is much more informative to display the data in isochronal plots vs. temperature. Dielectric constant and

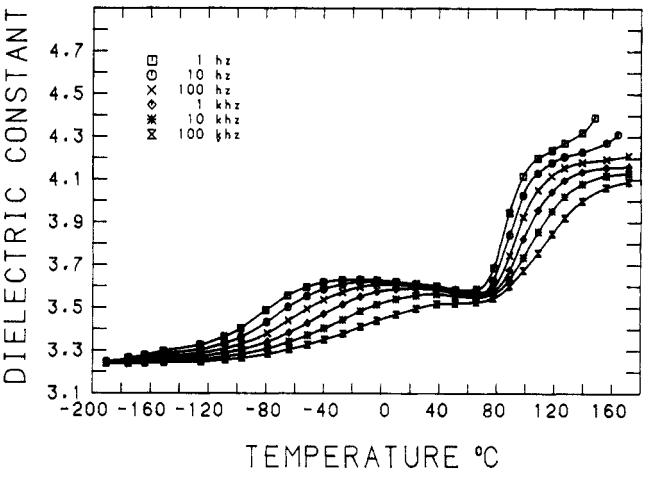

Figure 3. Dielectric constant of crystalline PET (sample 6, Table I, χ_c = 0.50) vs. temperature at six decade frequencies.

loss data at six decade frequencies (intermediate ones are omitted for clarity of display) are shown in Figures 1 and 2 for the "amorphous" sample and Figures 3 and 4 for a crystalline one (50%). The α_a and β processes are easily discerned in the same isothermal plot. Two other features deserve comment. Onset of crystallization in the amorphous sample at 100 °C is clearly evident in the data as a drop in the dielectric constant (due to reduction in the amorphous content) and by what appears to be a new loss peak at higher temperature. The latter is due to displacement of the loss process in the crystalline material. The coexistence of separate loss peaks for the unconstrained amorphous phase in as yet uncrystallized material and for the constrained amorphous fraction between the crystal lamellae in already crystallized material has been

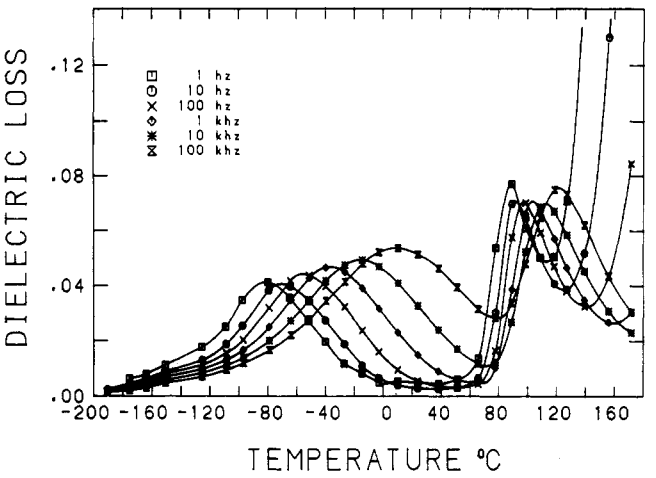

Figure 4. Dielectric loss of crystalline PET (sample 6, Table I, $\chi_c = 0.50$) vs. temperature at six decade frequencies.

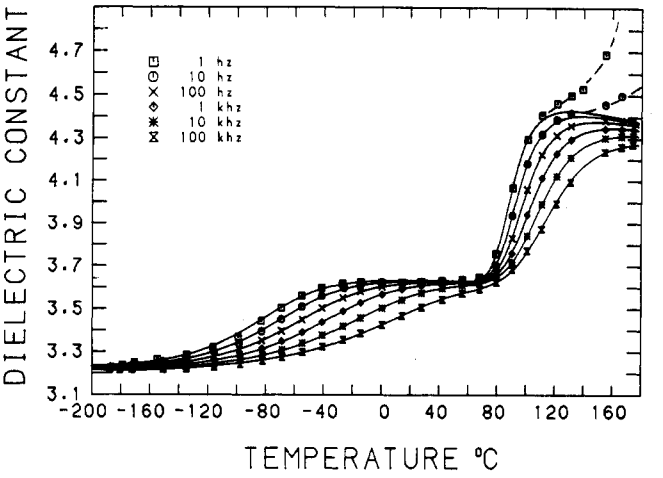

Figure 5. Havriliak–Negami phenomenological equation fit of the dielectric constant of sample 5, $\chi_c = 0.38$, using the parameters of Tables II and III. Dashed curves show the Maxwell–Wagner–Sillars polarization region, which was not fit.

studied by Tidy and Williams (as reported by Williams[16]). In the crystalline sample (Figures 3 and 4) the higher temperature behavior shows the presence of Maxwell–Wagner–Sillars polarization (rising dielectric constant and loss with temperature) as a result of the conductance in a two-phase crystalline/amorphous system.

In order to reach conclusions concerning the questions outlined in the Introduction, derived quantities such as relaxed and unrelaxed dielectric constants and relaxation strengths for the separate α_a and β processes will be required. To accomphish this we have fit the Havriliak–Negami[17] phenomenological equation to our data. This equation is a generalization that incorporates both the symmetric broadening of the Cole–Cole equation[18] and the asymmetric broadening of the Davidson–Cole[19] equation. The complex dielectric constant increment, $\Delta\epsilon^*$, is expressed as

$$\Delta\epsilon^* = (\epsilon_R - \epsilon_U)(1 + (i\omega\tau_0)^{\alpha'})^{-\beta'} \quad (1)$$

where R and U refer to relaxed and unrelaxed values of the dielectric constant, α' is the symmetric broadening parameter, β' is the asymmetric broadening parameter, τ_0 is the central relaxation time, and ω is angular frequency. The complete complex dielectric constant, ϵ^*, was assumed to be the sum of two increments expressed as in eq 1, one for each relaxation, α_a and β,

$$\epsilon^* = \Delta\epsilon^*(\alpha_a) + \Delta\epsilon^*(\beta) + \epsilon_U(\beta) \quad (2)$$

plus the unrelaxed dielectric constant for the lower temperature process. Equation 2 was fit globally to all of the data on a given specimen by parameterizing the quantities in eq 1 and 2 as functions of temperature. The relaxed and unrelaxed dielectric constants, ϵ_U and ϵ_R, and the α' width parameter were assumed to be linear functions of temperature (referred to an arbitrary temperature, T_0)

$$\epsilon_U = \epsilon_U^0 + S_U(T - T_0) \quad (3a)$$

$$\epsilon_R = \epsilon_R^0 + S_R(T - T_0) \quad (3b)$$

$$\alpha' = \alpha'_0 + \alpha'_1(T - T_0) \quad (3c)$$

The central relaxation time was taken to have, in general, Vogel–WLF temperature dependence

$$\log \tau_0 = A/(T - T_\infty) + B \quad (4)$$

Only for the α_a process in the amorphous sample was it found appropriate to invoke the asymmetric broadening parameter ($\beta' < 1$), and in this case it was kept temperature

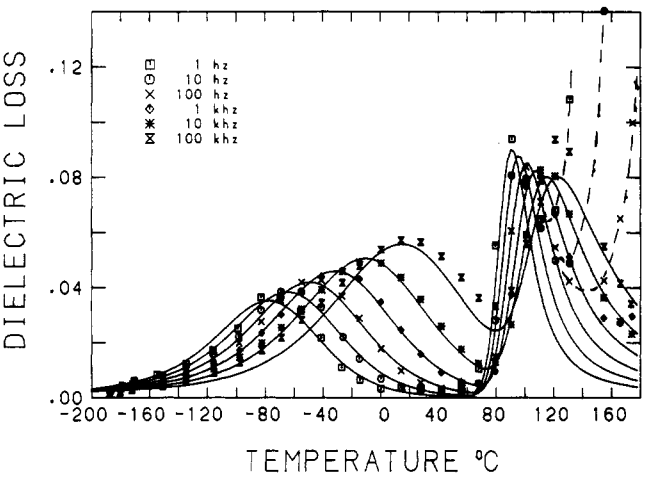

Figure 6. Havriliak–Negami phenomenological equation fit of the dielectric loss of sample 5, $\chi_c = 0.38$, using the parameters of Tables II and III. Dashed curves show the Maxwell–Wagner–Sillars polarization region, which was not fit.

independent. Consistency requires that $\epsilon_U(\alpha) = \epsilon_R(\beta)$. However, it was found that a better fit could be obtained if S_R in eq 3b for the β process was allowed to have a different value in the temperature region dominated by the α_a process. A crossover temperature, T', between the regions was selected above which S_R was optimized to a separate value. The parameter determination was carried out as follows. Initial estimates for ϵ_R, ϵ_U, α', and τ_0 (and β' in the case of the amorphous-sample α_a process) were obtained from isothermal plots at 5 °C intervals of ϵ'' vs. ϵ' (Argand diagrams). The 5 °C interval data were taken from cubic spline smoothing of the actual data. The parameters found at each temperature were then fit to eq 3a–c and 4. It was apparent at this point that good fits of log τ_0 for the β process were achieved with $T_\infty = 0$ (Arrhenius behavior). The parameters (with the exception of β' and T_∞, which were not further adjusted) were then improved by optimization via the least-squares fit of the calculated curves to the data. This was accomplished by an iterative Newton–Raphson technique.[20] In carrying this out we found it more effective to optimize first the β-process parameters with the α_a ones constrained to initial values. Then the α_a parameters were optimized with the β ones constrained. The optimized parameters are listed in Tables II and III. An example of the fits achieved to ϵ' and ϵ'' is shown in Figures 5 and 6 (38% crystalline

Table II
Relaxation Parameters for the β Process[a,b]

	ϵ_U		ϵ_R			α'			log τ		
sample	ϵ_U^0	$S_U \times 10^2$	ϵ_R^0	$S_R \times 10^2$	T'	α_0'	$\alpha_1' \times 10^2$	β'	A	$-B$	T_∞
1	3.177	0.0276	3.838	0.0227		0.0433	0.1514	1.0	2838	15.91	0.0
2	3.263	0.0010	4.147	−0.1483	347.2	0.0334	0.1255	1.0	3357	18.00	0.0
3	3.195	−0.0045	4.145	−0.1858	348.7	0.0118	0.1286	1.0	3500	18.61	0.0
4	3.145	0.0354	3.662	−0.0076		−0.0111	0.1695	1.0	2781	15.73	0.0
5	3.171	0.0429	3.668	−0.0144	339.8	−0.0144	0.1776	1.0	2787	15.73	0.0
6	3.211	0.0175	3.888	−0.1240		−0.0062	0.1552	1.0	3253	17.79	0.0
7	3.106	0.0325	3.554	−0.0537	331.0	−0.0103	0.1740	1.0	2830	15.99	0.0
8	3.155	0.0225	3.435	0.0102	335.1	−0.0089	0.1737	1.0	2457	14.71	0.0
9	3.191	−0.0288	3.379	0.0117	313.0	0.0291	0.1211	1.0	2185	14.19	0.0

[a] T_0 = 73.0 K for all samples. [b] For $T > T'$, $\epsilon_R = \epsilon_U$ from Table III.

Table III
Relaxation Parameters for the α_a Process[a,b]

	ϵ_U			ϵ_R		α'			log τ		
sample	ϵ_U^0	$S_U \times 10^2$	T'	ϵ_R^0	$S_R \times 10^2$	α_0'	$\alpha_1' \times 10^2$	β'	A	$-B$	T_∞
1	3.838	0.0227		6.053	−1.8055	0.8097	0.2696	0.3	230.6	9.04	327.25
2	2.972	0.2800	347.2	4.923	−0.2485	0.3150	−0.0633	1.0	855.0	14.35	306.25
3	2.840	0.2872	348.7	4.672	−0.0556	0.2915	−0.0257	1.0	968.4	15.20	303.85
4	3.662	−0.0076		4.540	0.0000	0.2620	0.0000	1.0	914.4	14.98	303.15
5	3.250	0.1423	339.8	4.552	−0.1605	0.2691	−0.5202	1.0	884.6	14.47	300.0
6	3.888	−0.1240		4.336	−0.1054	0.2189	−0.0213	1.0	861.5	14.87	300.0
7	3.150	0.1027	331.0	4.060	−0.0247	0.2278	−0.0100	1.0	858.2	14.33	300.0
8	2.875	0.2236	335.1	4.003	−0.0976	0.3288	−0.1990	1.0	610.6	10.77	300.0
9	3.094	0.1305	313.0	3.936	0.2524	0.2782	−0.1742	1.0	488.1	9.43	300.0

[a] T_0 = 73.0 K for ϵ_U and ϵ_R; T_0 = 350.0 K for $\bar{\alpha}$. [b] For $T < T'$, $\epsilon_U = \epsilon_R$ from Table II.

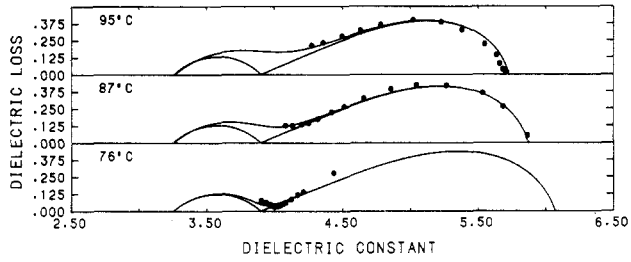

Figure 7. Argand diagrams (Cole–Cole plots) for "amorphous" PET (sample 1, Table I, χ_c = 0.04) in the temperature region of the α_a process. Curves are calculated from the Havriliak–Negami equation and the parameters of Tables II and III. Calculated curves for the separate α_a and β processes are also shown.

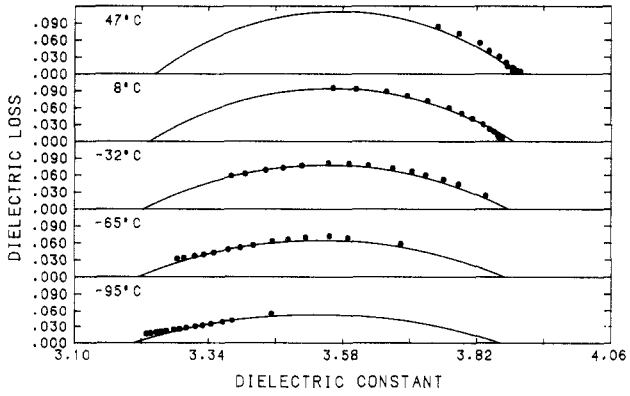

Figure 8. Argand diagrams (Cole–Cole plots) for "amorphous" PET (sample 1, Table I, χ_c = 0.04) in the temperature region of the β process. Curves are calculated from the Havriliak–Negami equation and the parameters of Table II.

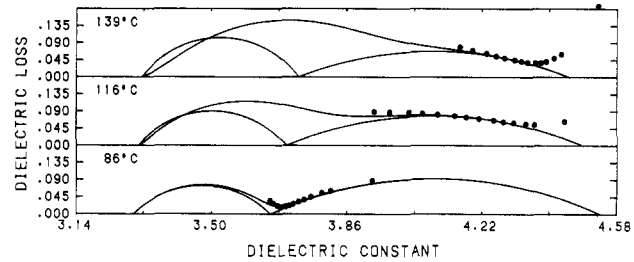

Figure 9. Argand diagrams (Cole–Cole plots) for crystalline PET (sample 5, χ_c = 0.38 in the temperature region of the α_a process. Curves are calculated from the Havriliak–Negami equation and the parameters of Tables II and III. Calculated curves for the separate α_a and β processes are also shown.

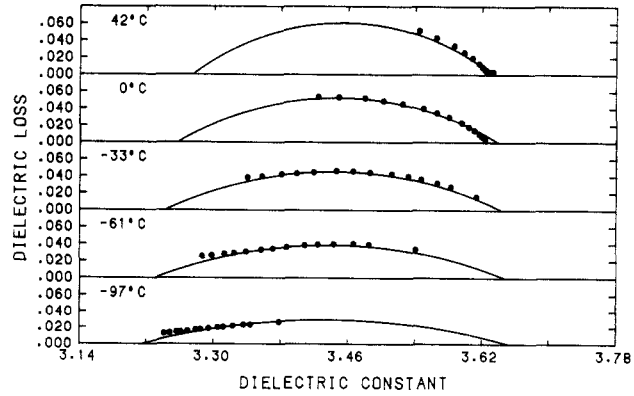

Figure 10. Argand diagrams (Cole–Cole plots for crystalline PET (sample 5, χ_c = 0.38) in the temperature region of the β process. Curves are calculated from the Havriliak–Negami equation and the parameters of Table II.

sample). No attempt to fit the Maxwell–Wagner–Sillars polarization was made, and the experimental points in the dashed regions of these figures were unweighted in the fitting. Comparisons of calculated and experimental Argand diagrams for the amorphous sample are shown in Figures 7 and 8 for the α_a and β regions, respectively, and for the 38% crystalline sample in Figures 9 and 10. Comparison of the α' width parameters as a function of temperature for both relaxations for all of the specimens is made in Figure 11. Similar comparison is made of the central relaxation times (vs. reciprocal temperature) in Figure 12.

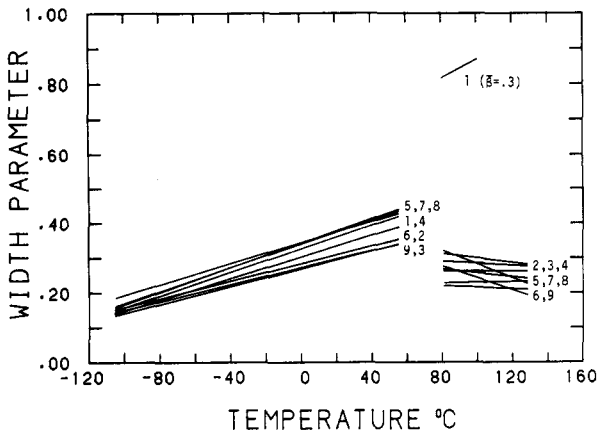

Figure 11. α' width (symmetric broadening) parameters (Havriliak–Negami equation) vs. temperature for the α_a and β processes. The numbers refer to the samples of Table I. Only for the amorphous-sample (sample 1) α_a process was the β' skewing parameter invoked (i.e., $\beta' < 1$); its value is recorded on the plot next to the α' curve.

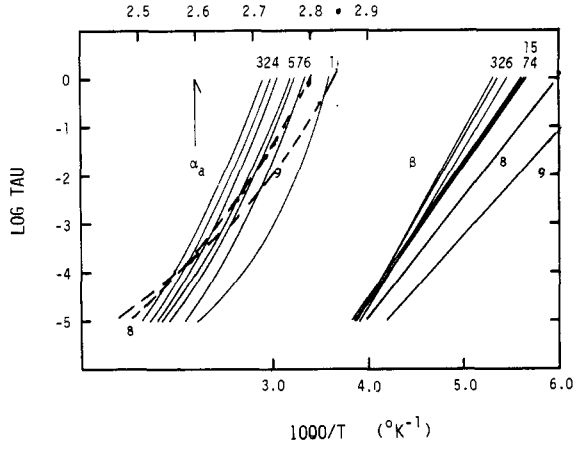

Figure 12. Temperature dependence of the central relaxation times for the α_a and β processes. The numbers refer to the samples of Table I.

Discussion

Relaxation Parameters and Crystallinity. Some comments on the general morphological dependence of the relaxation parameters are in order. The dramatic differences between the amorphous and crystalline specimens in the relaxation shape and width of the α_a glass–rubber relaxation are evident in the Argand diagrams of Figures 7 and 9 and the α' width parameter plots of Figure 11. The relaxation is much narrower and skewed in the amorphous sample in comparison with the apparently symmetric extremely broad process in the crystalline ones. These differences appear to be common to the comparison of the glass–rubber relaxations in amorphous polymers with those in semicrystalline ones.[5] From inspection of Figure 11 there appear to be no consistent differences among the crystalline samples with respect to the width of the α_a process. The temperature dependence of the central relaxation time for the α_a relaxation (Figure 12) shows that the process is displaced to higher temperature in the crystalline samples. Illers and Breuer[4] noticed a progression of T_{max} for the G'' loss peak to higher temperature with increasing crystallinity at the lower crystallinities followed by reversal of the trend at higher crystallinity. The same trend is noticeable in our data (Figure 12). The two highest crystallinity samples show overall slopes somewhat lower than the others. Illers and Breuer attributed the reversal effect to the amorphous layer increasing in thickness at higher crystallinity along with crystal thickness. This presumably would lessen the amorphous-phase immobilization by the crystals. Turning to the β process, one sees upon comparing the Argand diagrams for the amorphous PET (Figure 8) with those for a crystalline specimen (Figure 10) that in both cases the relaxation is extremely broad and apparently symmetric. It may be seen in Figure 11 that there is no consistent trend with respect to the Cole–Cole α' width parameters among the specimens, *including the amorphous one*. In Figure 12 it is seen that with the exception of the one or two highest crystallinity samples there is little difference or trend with respect to the temperature dependence of central relaxation time, including the amorphous sample. The overall independence of the behavior of the β process of morphological factors, even to the extent of being insensitive to whether or not the crystal phase is present, appears to be characteristic of subglass relaxations in general.[5]

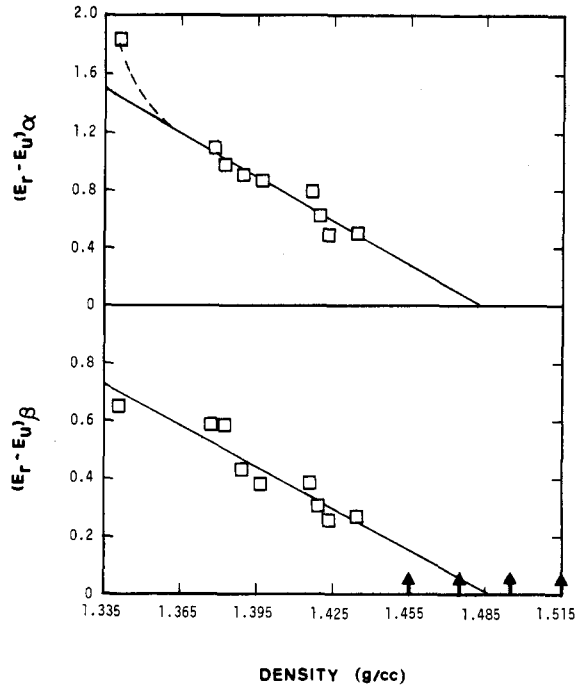

Figure 13. Extrapolation of relaxation strength vs. crystallinity for the α_a (upper panel, at 90 °C) and β (lower panel, at 20 °C) processes. The four arrows on the density abscissa refer to four crystal densities from the literature as discussed in the text.

Extrapolation of Relaxation Strengths vs. Crystallinity. Relaxation strengths, $(\epsilon_R - \epsilon_U)$, for the α_a and β processes in each of the specimens may be calculated from the relaxed and unrelaxed dielectric constants listed in Tables II and III. These are plotted vs. density in Figure 13. From the appearance of the data, linear extrapolation of the β process to high crystallinity seems appropriate. The same would seem to be true of the α_a data, excluding that for the amorphous sample. Quite significantly, these extrapolations reach zero strength at the same density for both processes (and at the midpoint of the ranges of the reported crystal densities). Since there seems to be no doubt of the entirely amorphous character of the α_a relaxation, it is to be concluded that the β relaxation must be of entirely amorphous origin also. Comments on the linear nature of the extrapolation are in order. It is profitable to view the dielectric constant from the point of view of a two-phase composite of crystalline and amorphous phases each with its own dielectric constant. If the dielectric constants of the two phases are independent of crystallinity, then it is easly to show[21] that for

relaxation strengths as small as those for the β process (relative to the unrelaxed constants), the composite mixture dielectric constant should be a linear function of volume fraction of the phases (crystallinity). Since the relaxational parameters for the β process show a strong tendency for independence of crystallinity, it is reasonable that the phase dielectric constants would be also. Thus linear extrapolation of the β-process relaxation strength is not unexpected. Much of what is said regarding the β-process extrapolation is true of the α_a one, excluding the amorphous sample. The latter material, as indicated, has significantly different behavior with respect to the other α_a relaxation parameters as well. As was determined in the calculations presented in the next section concerning the dipolar correlation factor, its dielectric constant is also significantly different from that of the amorphous phase in the semicrystalline samples. Returning to the results of the extrapolation, it is interesting to note that the extremes of the four crystal densities discussed above under sample charcterization appear inconsistent with the dual extrapolation of Figure 13 and that the relaxation data itself lends support for a value near the two middle densities.

Influence of Crystallinity on the Correlation Factor for Amorphous-Phase Dipole Relaxation. The calculation of the dipolar relaxation correlation factor in semicrystalline polymers is best accomplished in two steps. First, by considering the material to be a two-phase composite, one can calculate the amorphous-phase dielectric constant from the measured specimen value and a knowledge of the crystal-phase dielectric constant. Then the correlation factor can be calculated from the derived amorphous-phase dielectric constant by the Onsager–Kirkwood equation. The first step requires a composite model for the dielectric constant. In the present case, an adequate model exists in the form of bounds on the dielectric constant of locally lamellar structures.[21] In the case of lamellae distributed isotropically on the macro scale the bounds are

$$\epsilon_U = (\epsilon_V + 2\epsilon_H)/3 \tag{5a}$$

$$1/\epsilon_L = (1/\epsilon_V + 2/\epsilon_H)/3 \tag{5b}$$

where ϵ_U and ϵ_L are upper and lower bounds on the specimen dielectric constant, ϵ_V and ϵ_H are given by

$$\epsilon_H = v_1\epsilon_1 + v_2\epsilon_2 \tag{5c}$$

$$1/\epsilon_V = v_1/\epsilon_1 + v_2/\epsilon_2 \tag{5d}$$

and ϵ_1, ϵ_2, v_1, and v_2 refer to the dielectric constants and volume fractions of the amorphous (1) and crystalline (2) phases. By equating specimen dielectric constant values from Tables II and III to ϵ_U and ϵ_L in eq 5a,b and knowing the crystal-phase constant ϵ_2, one can back-calculate lower and upper bound estimates of ϵ_1 from eq 5c,d. For the dielectric constants encountered here, the derived lower and upper bound values of ϵ_1 are identical to within practical accuracy. The crystal-phase dielectric constant was assumed to be equal to the specimen $\epsilon_U(\beta)$ value but with a density correction from specimen density to the crystal density using the Clausius–Mosotti relation.[22] With the amorphous-phase dielectric constants established, the Onsager–Kirkwood equation[23] can be used to calculate the correlation factor. A dipole moment of 1.89 D was used.[24] The calculation of the correlation factor was carried out separately for the β process (from $\epsilon_R(\beta)$) and the combined α_a and β processes (from $\epsilon_R(\alpha_a)$). The results are displayed in Figure 14. The correlation factor can be thought of as responding to two types of influences. The first is the direct correlation with nearby dipoles and dominated by

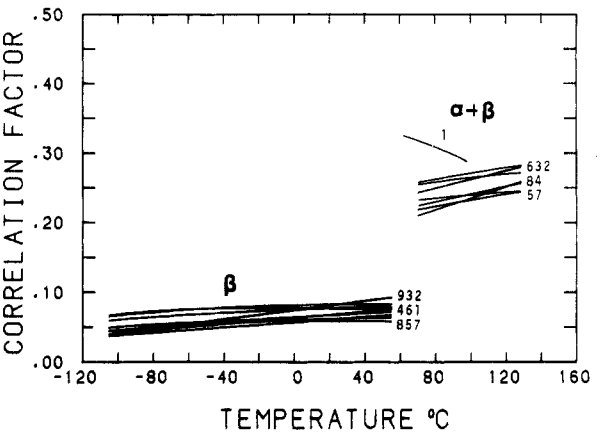

Figure 14. Dipolar correlation factors (calculated from the Onsager–Kirkwood equation) for the β and (α_a + β) processes. The numbers refer to the samples of Table I.

intramolecular correlation. The relatively low value for the correlation factor (α_a + β) of the amorphous sample (vincinity of 0.3) is due to intramolecular correlation. The dipole moment of the two ester groups attached to the same benzene rings partially cancels and the degree of cancellation depends on the relative population of cis and trans conformations of the two ester groups with respect to each other. Another contribution to the correlation factor can arise from the spatial ability of dipoles to reorient. Restriction of spatial freedom of orientation can lead to lowering of the correlation factor. Since more configurations become available with increasing temperature, spatial restriction is likely to lead to a positive temperature coefficient for the correlation factor. It is to be noticed that the correlation factors for the crystalline specimens are significantly less than for the amorphous sample and that the temperature coefficient is positive. It is probable that this is the result of the restriction in availability of conformations due to the connections of the chain segments in the amorphous fraction to the crystals. Thus it can be concluded that immobilization of the amorphous fraction by the crystals not only perturbs the relaxation times but noticeably affects the accessiblity of configurations as well.

The temperature-dependent immobilization of the amorphous fraction is also observable via NMR measurements.[25] A "more mobile" and a "less mobile" amorphous fraction have been invoked in the interpretation of NMR results. The "less mobile" amorphous fraction has been found to increase with temperature. In this context, it is perhaps worth commenting that the dielectric relaxation spectrum associated with the α_a relaxation can be inferred rather directly from frequency measurements covering six decades. As indicated, it is greatly broadened in the semicrystalline environment but it is a continuous spectrum showing no structure attributable separately to the morphological entities giving rise to the broadening. The latter would include tight and loose folds and chains confined by association with an interface. It can be speculated that were a more complete spectral density function available from the NMR studies it would show the same broad continuous structure and that the division into discrete fractions is a useful first approximation. It may be seen that for the β process the correlation factors are very similar for the various specimens and that there is no apparent correlation with the values and the degree of crystallinity. This is consistent with the general lack of morphological sensitivity of the β process commented on earlier. The relatively small numerical values of the

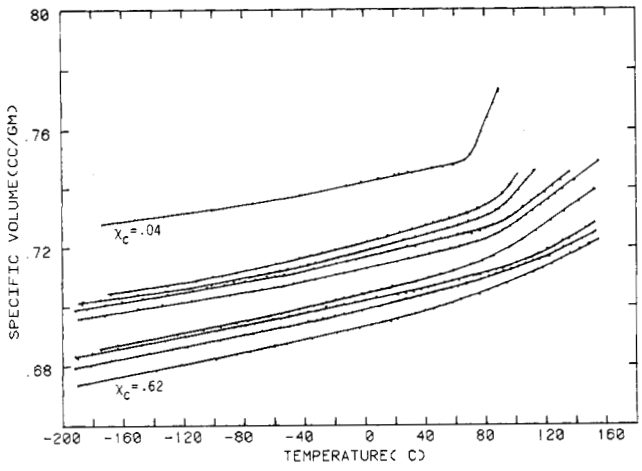

Figure 15. Specific volume vs. temperature for the nine samples of table I.

correlation factor (~0.05) can be due to small but finite spatial reorientational ability of all amorphous polar groups or to a small number that have considerable reorientational ability and the rest being effectively completely restricted. It is not possible to distinguish these two extreme mechanisms for the β process on the basis of relaxation strength measurements alone.

Specific Volume vs. Temperature. Plots of specific volume vs. temperature for the various specimens are shown in Figure 15. These were constructed from the room-temperature densities of Table I and the linear thermal expansion measurements in the dielectric cell under the assumption that the expansion is isotropic. The abrupt change in thermal expansion coefficient through the glass transition in the amorphous specimen is readily apparent (the actual value of the slope above T_g is probably not reliable for a completely amorphous material due to its becoming fluid). The thermal expansion change in the crystalline specimens is progressively less with increasing temperature as expected from the composite nature of the semicrystalline material and the decreasing amorphous fraction. In addition, however, it appears that the temperature interval over which the thermal expansion changes is wider in the crystalline specimens and the glass transition more diffuse. This of course is consistent with the broadening observed in the dielectric α_a relaxation process with the onset of crystallinity. There also is a thermal expansion change in the β region (~−80 °C). In the amorphous sample the change is not as nearly as great and is more diffuse in comparison with that associated with the α_a process. The diffuse nature is to be expected on the basis of the broad β process found dielectrically. Due to the decreasing amorphous fraction the thermal expansion change can no longer be reliably detected in the higher crystallinity samples.

Acknowledgment. We are grateful to the Polymers Program, Division of Materials Research, National Science Foundation for financial support of this work.

Registry No. PET, 25038-59-9.

References and Notes

(1) Reddish, W. *Faraday Soc. Trans* **1949**, *46*, 549.
(2) Ishida, Y.; Yamafuji, K.; Ito, H.; Takayanagi, M. *Kolloid Z. Z. Polym.* **1962**, *184*, 97.
(3) Saito, S. *Kolloid Z. Z. Polym.* **1963**, *189*, 116.
(4) Illers, K. H.; Breuer, H. *J. Colloid Sci.* **1963**, *18*, 1.
(5) Boyd, R. H. *Polymer* **1985**, *26*, 323.
(6) Daubney, R. de P.; Bunn, C. W.; Brown, C. J. *Proc. R. Soc. London, Ser. A* **1954**, *226*, 531.
(7) Kilian, H. G.; Halboth, H.; Jenckel, E. *Kolloid-Z.* **1960**, *172*, 166.
(8) Fakirov, S.; Fischer, E. W.; Schmidt, G. F. *Makromol. Chem.* **1975**, *176*, 2459.
(9) Starkweather, H. W.; Zoller, P.; Jones, G. A. *J. Polym. Sci., Polym. Phys. Ed.* **1983**, *21*, 295.
(10) Yoshihara, M.; Work, R. N. *J. Chem. Phys.* **1980**, *72*, 5909.
(11) Ashcraft, C. R.; Boyd, R. H. *J. Polym. Sci., Polym. Phys. Ed.* **1976**, *14*, 2153.
(12) Seigmann, A.; Harget, P. J. *J. Polym. Sci., Polym. Phys. Ed.* **1980**, *18*, 2181.
(13) Mehta, A.; Wunderlich, B. *J. Polym. Sci., Polym. Phys. Ed.* **1978**, *16*, 289.
(14) Hiramatsu, N.; Hirakawa, S. *Polymer* **1980**, *12*, 105.
(15) Coburn, J. C. Ph.D. Dissertation, University of Utah, 1984.
(16) Williams, G. *Adv. Polym. Sci.* **1979**, *33*, 59.
(17) Havriliak, S.; Negami, S. *Polymer* **1967**, *8*, 161.
(18) Cole, K. S. Cole, R. H. *J. Chem. Phys*, 1941, *9*, 341.
(19) Davidson, D. W.; Cole, R. H. *J. Chem. Phys.* **1950**, *18*, 1417.
(20) Boyd, R. H. In *Computer Applications in Applied Polymer Science*; Provder, T., Ed.; American Chemical Society: Washington, DC, 1986; ACS Symp. Ser. No. 313.
(21) Boyd, R. H. *J. Polym. Sci., Polym. Phys. Ed.* **1983**, *21*, 505.
(22) Smyth, C. P. *Dielectric Behavior and Structure*; McGraw-Hill: New York, 1955.
(23) Froelich, H. *Theory of Dielectrics*, 2nd ed.; Oxford University: Oxford, 1958.
(24) Saiz, E.; Hummel, J. P.; Flory, P. J.; Plavslc, M. *J. Phys. Chem.* **1981**, *85*, 3211.
(25) English, A. D. *Macromolecules* **1984**, *17*, 2182. This paper also contains extensive references to previous NMR work on PET.